Spectrochimica Acta Part A: Molecular and Biomolecular Spectroscopy 110 (2013) 72–77

Contents lists available at SciVerse ScienceDirect

Spectrochimica Acta Part A: Molecular and Biomolecular Spectroscopy

journal homepage: www.elsevier.com/locate/saa

Synthesis of hollow gold nanoparticles on the surface of indium tin oxide glass and their application for plasmonic biosensor

Tingting Hu, Yuanyuan Lin, Jilin Yan, Junwei Di *

The Key Lab of Health Chemistry and Molecular Diagnosis of Suzhou, College of Chemistry, Chemical Engineering and Material Science, Soochow University, Suzhou, Jiangsu 215123, PR China

HIGHLIGHTS

- Hollow gold nanoparticles have been synthesis on the surface of indium tin oxide glass substrate.
- The surface plasmon peak of hollow gold nanoparticles was red-shifted to near infrared region.
- The "clean" gold surface can be tailored easily for functionalize special molecules.
- These nanoparticles were applied to fabrication of biosensors based on the plasmonic resonance.

GRAPHICAL ABSTRACT

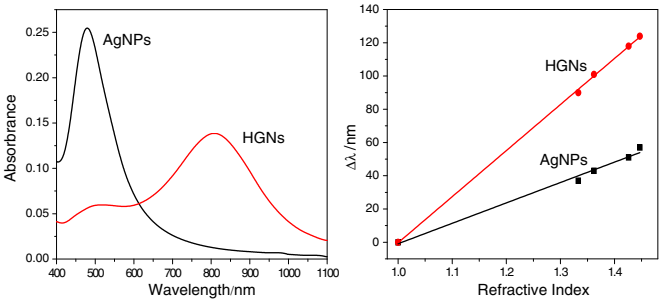

ARTICLE INFO

Article history:
Received 12 December 2012
Received in revised form 14 February 2013
Accepted 3 March 2013
Available online 14 March 2013

Keywords:
Hollow gold nanoparticles
Localized surface plasmon resonance
Near-infrared
Biosensor

ABSTRACT

Hollow gold nanoparticles (HGNs) deposited on the surface of transparent indium tin oxide (ITO) glass have been synthesized. The silver nanoparticles were firstly electrodeposited directly on the ITO surface as a template without any organic ligands or surfactants. Then these silver nanoparticles were taken as sacrificial templates and the HGNs were obtained by Galvanic replacement reaction between $HAuCl_4$ solution and silver nanoparticles. The localized surface plasmon resonance (LSPR) peak of HGNs was located at near infrared region of ~800 nm, which was largely red-shifted as compared to silver nanoparticles as a template. Moreover, the refractive index sensitivity of HGNs was enhanced to 277 nm per refractive index unit, which was also much higher than that of silver nanoparticles deposited on ITO substrate. The "clean" surface of HGNs could be further functionalized by special biomolecules and applied to fabrication of LSPR biosensors. This approach provides a potential opportunity as LSPR biosensors for chemical or biological analysis especially on tissue and blood samples.

Introduction

In recent years, noble metal nanoparticles are particularly interesting for chemical and biological sensing applications due to the rich and tunable local surface plasmon resonance (LSPR) properties [1–3]. The LSPR position of the nanoparticles in wavelength is dependent on the composition, the size and shape, nanoparticle interactions, and the environment surrounding the nanoparticles [4–6]. It is this last characteristic of the LSPR that has attracted the most interest and research effort since the binding of specific molecules onto the metal nanoparticle surface can cause a shift in the absorption band of the LSPR due to changes in their local dielectric environments. Thus, a simple sensing method was developed by combining LSPR of metal nanoparticles with a basic spectrophotometer [7–9].

In general, the LSPR peak center for gold spherical nanoparticles is located at around 520 nm. Moreover, the LSPR bands of gold nanostructures can be turned to absorb light wavelength in the visible to the near-infrared region (NIR) from different gold morphologies, such as rods, stars, nanoshells and hollow nanoparticles [10,11]. Among them, hollow gold nanoparticles (HGNs) are

* Corresponding author. Tel.: +86 512 65880354; fax: +86 512 65880089.
E-mail address: djw@suda.edu.cn (J. Di).

1386-1425/$ - see front matter © 2013 Elsevier B.V. All rights reserved.
http://dx.doi.org/10.1016/j.saa.2013.03.024

unique composite nanoparticles that consist of a thin gold shell with a hollow central. HGNs typically exhibit high surface areas, low densities, and tunable LSPR features. Practically, the peak LSPR band of HGNs is typically shifted to much longer wavelengths than the plasmon resonance of corresponding solid metal nanoparticles. This is much favorable for the construction of LSPR biosensors: (1) The NIR region between the spectrum of 700–1300 nm is optimal for optical transmission through tissues and blood [12–14]. It provides an opportunity to construct LSPR biosensors for application in protein sensing and cellular analysis in diluted whole blood. (2) The refractive index (RI) sensitivity is largely dependent on the LSPR band position of metal nanoparticles in a homogeneous dielectric environment [15]. The red-shifted LSPR band position would exhibit higher RI sensitivity. (3) Compared with a solid nanoshell with silica or gold sulfide core, a hollow gold nanostructure exhibits higher RI sensitivity with the same resonance wavelength [15].

The template-assisted approach provides a convenient and versatile method for the construction of hollow gold nanostructures [16]. Recently, Xia and co-workers developed a galvanic replacement reaction method for the synthesis of hollow gold nanocages [17,18]. Generally, silver nanoparticles are taken as sacrificial templates and their reaction with $HAuCl_4$ leads to the formation of gold shell with hollow center, in which the morphology of the silver core directly controls that of the resulting gold shells. Moreover, it has demonstrated that the LSPR of HGNs presented a much more sensitive response toward environmental changes compared with solid gold colloids with the similar size [17]. However, chemical analysis using metal nanoparticles suspended in a liquid solution suffers from the inherent stability of the colloidal system. The development of LSPR sensors based on the metal nanoparticles immobilized on solid support could provide good stability as well as consistent and stable response [19,20].

At present the most common strategy for immobilization of metal nanoparticles is self-assembled from colloidal solution onto a glass surface to obtain an optically transparent nanoparticles array using organic binder molecules of amine- or mercapto-terminated silanes [21]. In this system the metal nanoparticles are not free of the capping agents or stabilizers after immobilization from the liquid phase. This results in their surface somewhat more difficult for functionalization with specific receptors or ligands [21–23], which limits the applications in biological sensing. For example, the presence of cetyltrimethylammonium bromide (CTAB) on gold nanorod surface seriously hinders the application for construction of biosensors [22,24]. In this work, we firstly deposit the silver nanoparticles on the surface of indium tin oxide (ITO) film coated glass by the reduction of silver salts using electrochemical method. Subsequently, these silver nanoparticles are used as templates from which to grow hollow gold nanostructure using a chloroauric acid solution. The procedure avoids any organic stabilizers or surfactants. These "clean" HGNs can be tailored easily to functionalize the surface for construction of LSPR biosensors.

Experimental

Materials

ITO glass (1.1 mm thickness, 100 Ω) was purchased from Suzhou NSG Electronics Co., Ltd. (Suzhou, China). (3-Aminopropyl)trimethoxysilane (APTMS) were obtained from Sigma–Aldrich. The APTMS sol–gel solution was prepared by addition of 400 μL of APTMS and 332 μL of 0.1 M HCl into 33 mL of water with vigorous stir for at least 1 h [21]. Human-immunoglobulin G (h-IgG), goat anti-human-immunoglobulin G (anti-h-IgG), and biotin were commercially obtained from Chengwen Biotechnology (Beijing, China). Streptavidin (SA) was purchased from Beijing Boisynthesis Biotechnology Co., Ltd. (Beijing, China). Silver Nitrate ($AgNO_3$) and chloroauric acid ($HAuCl_4$) were products of Guoyao Chemical Regent Co., Ltd. All other chemicals were analytical pure. Twice-distilled water was used throughout the experiments.

Synthesis of HGNs on ITO substrate surface

The HGNs were prepared by first electrodepositing the silver nanoparticles onto ITO surface and then carrying out a galvanic replacement reaction between as-synthesizing silver nanomaterials and $AuCl_4^-$ ions. Typically, the ITO glass (3 × 0.6 cm) was washed with ammonia solution (1:20), ethanol and twice-distilled water for 10 min in an ultrasonic cleaner, respectively. The electrolyte consisted of 0.3 M $AgNO_3$ and 0.3 M KNO_3 solution kept at 30 °C. The solution was removed the air by high purity nitrogen gas for at least 10 min prior to electrolysis and maintained under nitrogen atmosphere during experiments. The silver deposition was performed by applying a cyclic voltammogram (CV) in the potential range of −0.15 to −0.45 V at 0.05 V/s for 100 cycles. After rinsed with water, the strips were immersed in 0.02 mM $HAuCl_4$ solution for 30 min at 50 °C. These prepared HGNs were rinsed by water and could be used to further modify the function interface.

Biotin-SA binding investigation

The prepared HGNs strips were modified by the formation of amino-functionalized surface, which was achieved by incubation of the strips in APTMS sol–gel solution for 2 h at room temperature and air-dried for 1 h. Then the strips were incubated in 0.2 mmol/L of biotin solution for 4 h followed by rinsing with water. In this process the amino-functionalized surface could interact with the carboxyl-group of biotin molecule. For the SA bind studies, the strips were left in SA and PBS solution for 2 h. The strips were rinsed with water and air-dried at room temperature before absorption measurement.

Antibody and antigen binding investigation

IgG-modified HGNs were obtained by chemical immobilization of the target protein directly on gold surface. The prepared HGNs strips were incubated in 100 μg/mL of anti-h-IgG in PBS solution (pH 7.4) for 12 h at 4 °C. Antibody and antigen binding events were examined by measurement of the UV–visible absorption spectra of the anti-h-IgG functionalized strips before and after incubation in h-IgG solution for 2 h.

Apparatus and measurements

Electrochemical depositions were performed with a CHI 830B electrochemical work station (CH Instruments Co., Shanghai, China). A three-electrode system comprising a bare ITO electrode as working electrode, a platinum wire as auxiliary electrode and a saturated calomel electrode (SCE) as reference was employed for electrolysis. The absorption spectrum was recorded at room temperature on a TU-2810 spectrophotometer (Beijing Purkinje General Instrument Co., Ltd.). Scanning electron microscopy (SEM) and energy dispersive X-ray spectroscopy (EDX) was obtained using S-4700 scanning electron microscope (Hitachi, Japan). X-ray diffraction (XRD) analysis was performed by X'Pert-Pro MPD (Panalytical, Holland).

Results and discussion

Preparation and characterization of HGNs onto ITO substrate

The AgNPs were deposited on transparent ITO glass surface using cyclic voltammetric method. Then HGNs were prepared

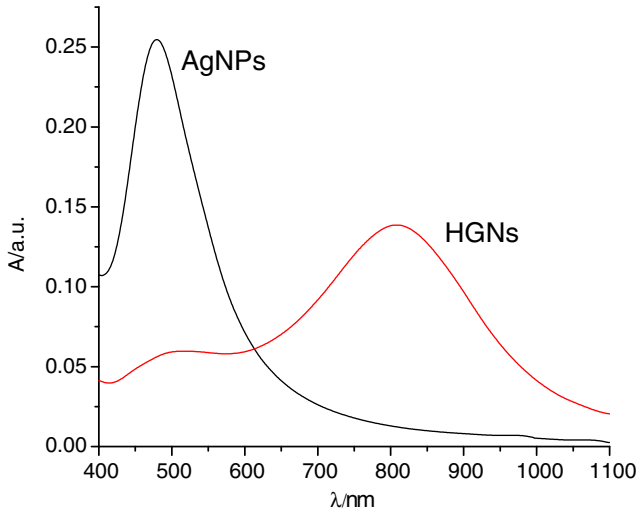

Fig. 1. UV–visible absorption spectra of metal nanoparticles on ITO surface in the air.

using the reaction of aqueous $HAuCl_4$ solutions with the AgNPs as templates. Fig. 1 shows the UV–visible absorbance spectra of AgNPs and HGNs deposited on ITO substrate against bare ITO glass as reference. The AgNPs exhibited a LSPR peak at about 480 nm. After reacted with aqueous $HAuCl_4$ solutions, the LSPR peak red-shifted to about 800 nm, which is consistent with that of HGNs on the previous reports [17,25,26]. This suggested that the HGNs were formed on the transparent ITO substrate surface. In fact, acquisition of NIR LSPR band of metal nanoparticles immobilized on the transparent substrate is crucial to fabrication of LSPR biosensors in this research.

Fig. 2A gives a typical SEM image of AgNPs that served as templates in the preparation of the HGNs. The nanoparticles were sparsely and randomly distributed on the surface of substrate without aggregation. The diameter of semi-spherical AgNPs was approximate 110 nm. These results indicate that the electrochemical reduction is regarded as a facile synthesis method to obtain large sized particles immobilized on solid substrate without any organic stabilizers and linkers. Fig. 2B shows an SEM image of the product after these AgNPs had reacted with $HAuCl_4$ solutions at 50 °C for 30 min. The elemental gold produced through Galvanic replacement reaction between metallic Ag and $HAuCl_4$ solution was covered onto the template surface. Assuming that all Ag templates was replaced to gold shell, the wall thickness of HGNs can be estimated to be ~5 nm (approximately one-tenth of the radius of the corresponding AgNPs) according to the stoichiometric relationship of replacement reaction [17]. As expected that the size of the particles was increased compared to the template of AgNPs. Moreover, a few fissures on the nanoparticles surface appeared. However, the pinholes or cavities on the nanoparticles are difficult to judge by SEM.

We used XRD and EDX to characterize the elemental composition of the HGNs formed by the replacement reaction. Fig. 2C displays the XRD pattern of AgNPs and HGNs. Only a weak band is observed at $2\theta = 38.1$ which corresponds to the (1 1 1) crystallographic planes due to the very thin silver film on substrate. For HGNs, a similar peak was observed at $2\theta = 38.5$, which corresponds to the (1 1 1) crystallographic planes. Fig. 2D shows the EDX spectrum of HGNs on the ITO substrate. The results indicate that the Au

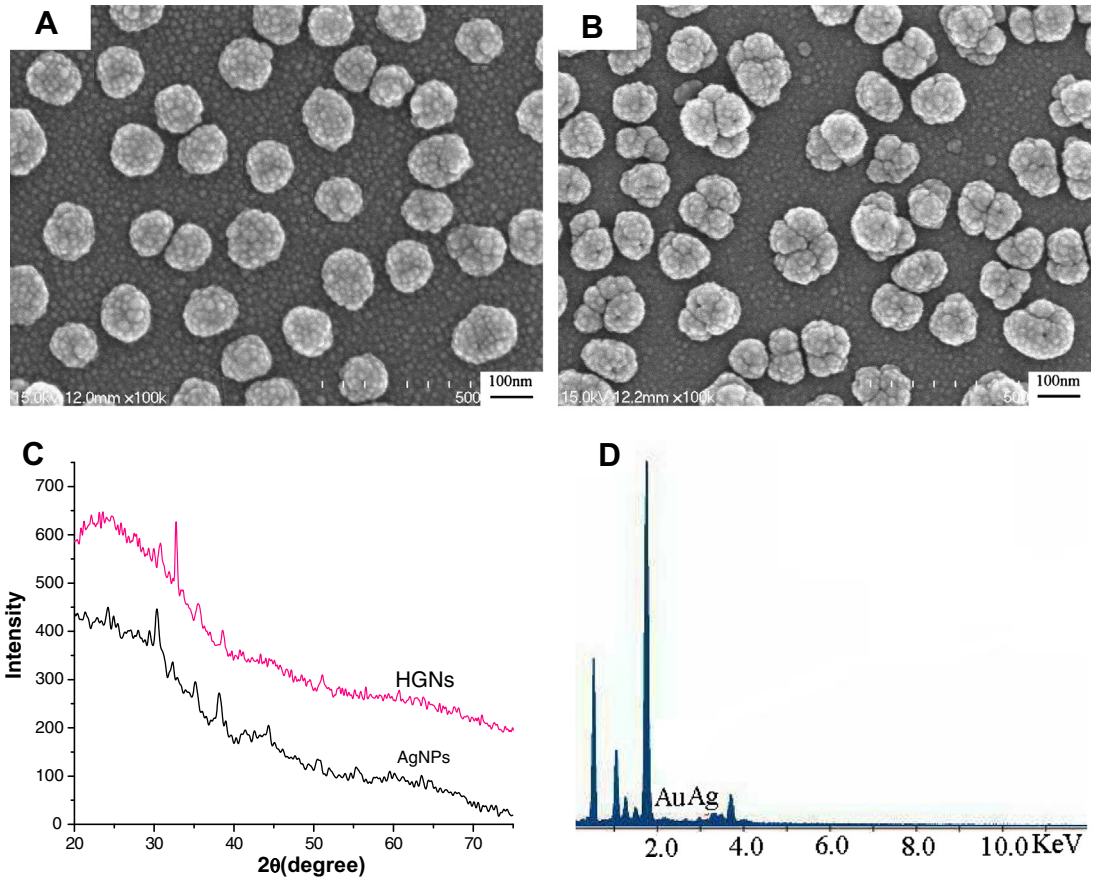

Fig. 2. SEM images of AgNPs (A) and HGNs (B) on the ITO surface, XRD pattern of metal nanostructures (C), and EDX spectrum of HGNs (D).

was deposited on the surface and Ag was partially dissolved from the interior.

The process of the HGN formation can be described as follows [13,17,25]: since the standard reduction potential of $AuCl_4^-$/Au (0.99 V vs SHE) is higher than that of Ag^+/Ag (0.8 V vs SHE), AgNPs immersed in the solution can be oxidized by $HAuCl_4$. The element gold begins to deposit on the template surface, which leads to the formation of an incomplete gold shell. At the same time, the Ag(0) core begins to oxidize and generates a hole or cavity on the nanoparticle surface. As gold deposits continuously on the surface, a larger cavity is generated in the interior with concomitant formation of Ag(I). When most of Ag core is dissolved, a gold nanoshell with a partial hollow cavity is produced.

Since gold and silver nanostructures exhibit distinctive LSPR peaks in the UV–visible region, we could conveniently monitor the replacement reaction between the AgNPs and $HAuCl_4$ solution using the spectroscopic method. Fig. 3A shows the absorption spectra recorded in the air when the AgNPs deposited on the transparent ITO substrate were reacted with different volumes of $HAuCl_4$ at 50 °C. The LSPR peak (~480 nm) of AgNPs continued to decrease in intensity as more $HAuCl_4$ was introduced. This peak became small after 1.0 mL $HAuCl_4$ solution had been added, indicating that the most of Ag was consumed. At the same time, a new LSPR band at NIR region appeared. This peak comes from the gold shell deposited on the template surface. The LSPR peak shifted to longer wavelength as the more volume of $HAuCl_4$ solution was added. However, the peak in intensity was highest after addition of 1.0 mL $HAuCl_4$ solution. The LSPR bands of HGNs produced by replacement reaction on silver templates were dependent on coverage and thickness of gold shell as well as silver core [13,27]. Therefore 1.0 mL of 0.1 mM $HAuCl_4$ solution was used in the following experiments.

Fig. 3B displays the UV–visible absorption spectra of the deposition AgNPs treated with 1.0 mL $HAuCl_4$ solution for various time at 50 °C. The LSPR peak (~480 nm) of AgNPs exhibited continuing decreases in the peak intensity upon increasing the immersion time. In the same case, the intensity of NIR LSPR peak (~800 nm) increased upon increasing the immersion time at beginning. The maximum LSPR peak appeared at the immersion of 30 min. Then the peak intensity decreased slowly upon the more immersion time. Therefore, the immersion time was selected to be 30 min in the experiments.

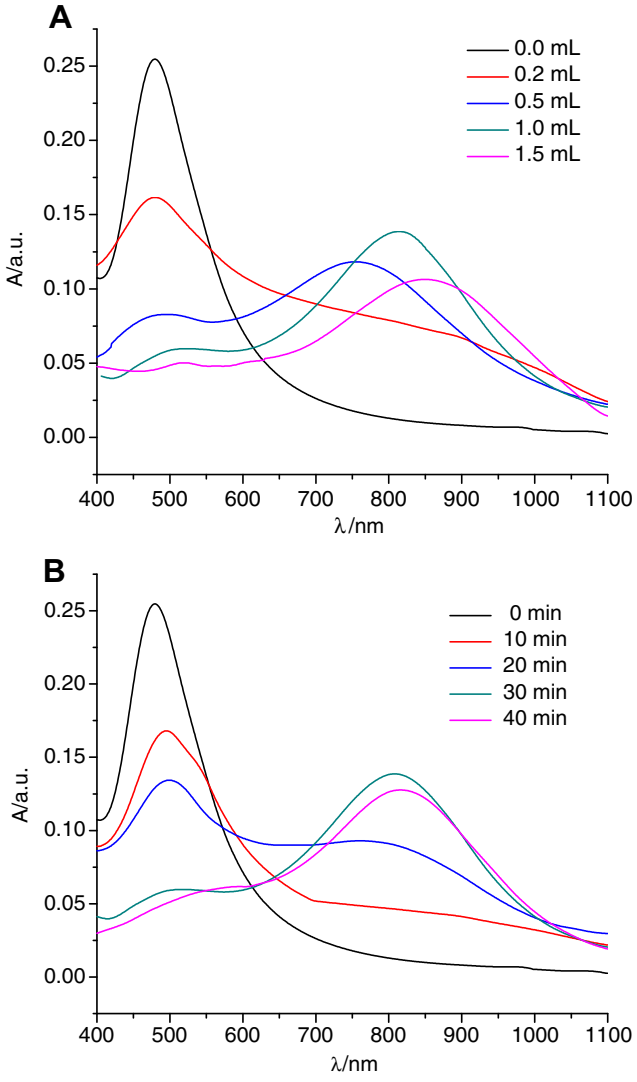

Fig. 3. UV–visible absorption spectra of AgNPs deposited on ITO surface in the air before and after had been treated by various volumes of 0.1 mM $HAuCl_4$ aqueous solution for 30 min in total volume of 5 mL (A) and by various time in 1 mL of $HAuCl_4$ aqueous solution (B).

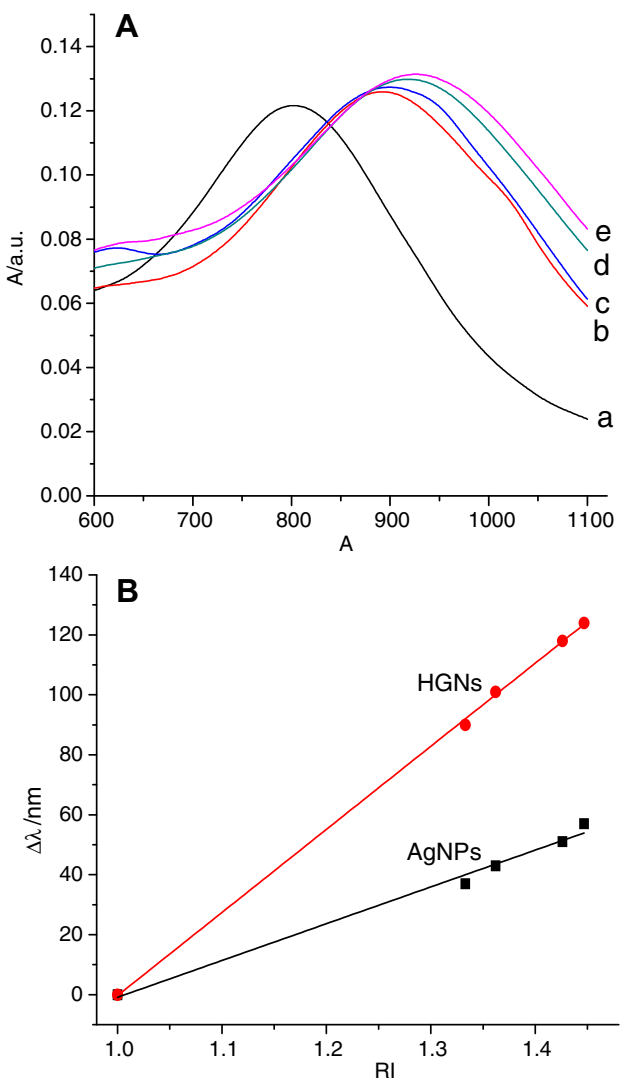

Fig. 4. UV–visible absorption spectra of HGNs in different solvent: (a) air; (b) water; (c) ethanol; (d) chloroform; (e) carbon tetrachloride (A). Calibration curves of the λ_{max} shift on the refractive index for LSPR of AgNPs and HGNs (B).

LSPR biosensors based on ITO/HGNs platform

We examined the ability of the ITO/HGNs strips to transduce changes in their surrounding media. UV–visible absorption spectra were recorded by immersing the ITO/HGNs strip in a series of solvent with different refractive indices. All of the LSPR peaks red-shifted as the RI of the solvent was increased (Fig. 4A). The relative shift in peak position was determined by taking the difference between the LSPR peak wavelength of metal nanoparticles in the solvent and in the air. It was observed that the relative wavelength shift was linearly dependent on the RI of the surrounding medium (Fig. 4B). From the slope of this plot, the RI sensitivity of the HGNs strip could be calculated as 277 nm/RIU. For comparison, the RI sensitivity of the AgNPs deposited on ITO substrate was 123 nm/RIU. This result indicates that the RI sensitivity of HGNs is much higher than that of the template of AgNPs.

The selectivity of a LSPR biosensor is enabled by the functionalization of molecules on the gold surface that target specific biological relevant species from solutions. To validate the feasibility of using the ITO/HGNs strip as a LSPR based biosensors, biotin and SA were used as model for receptor–analyte binding experiments. Fig. 5A shows the typical LSPR band shift after each step of surface modification in biotin-SA model bioassay. After modification of APTMS sol–gel film, a ~6 nm LSPR peak shift was observed. The binding of biotin cause a further LSPR peak shift ~4 nm. The final step was involved the binding of SA onto biotin. After binding of

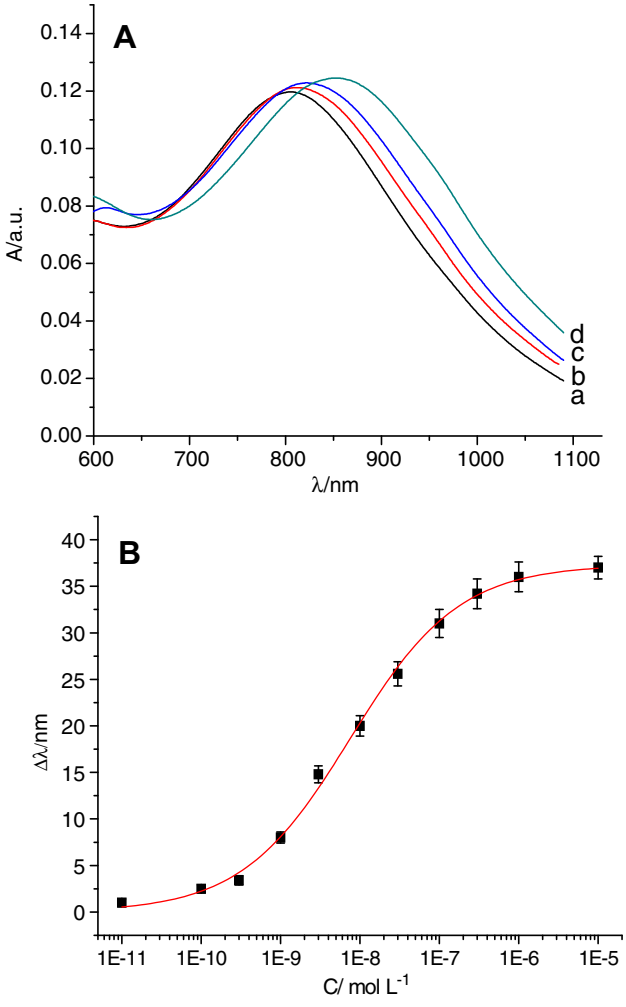

Fig. 5. UV–visible absorption spectra of HGNs before (a) and after incubated subseqently in AMTPS (b), biotin (c), and 1 μM of SA (d) solution (A). Relationship between the LSPR peak wavelength and the SA concentration (B).

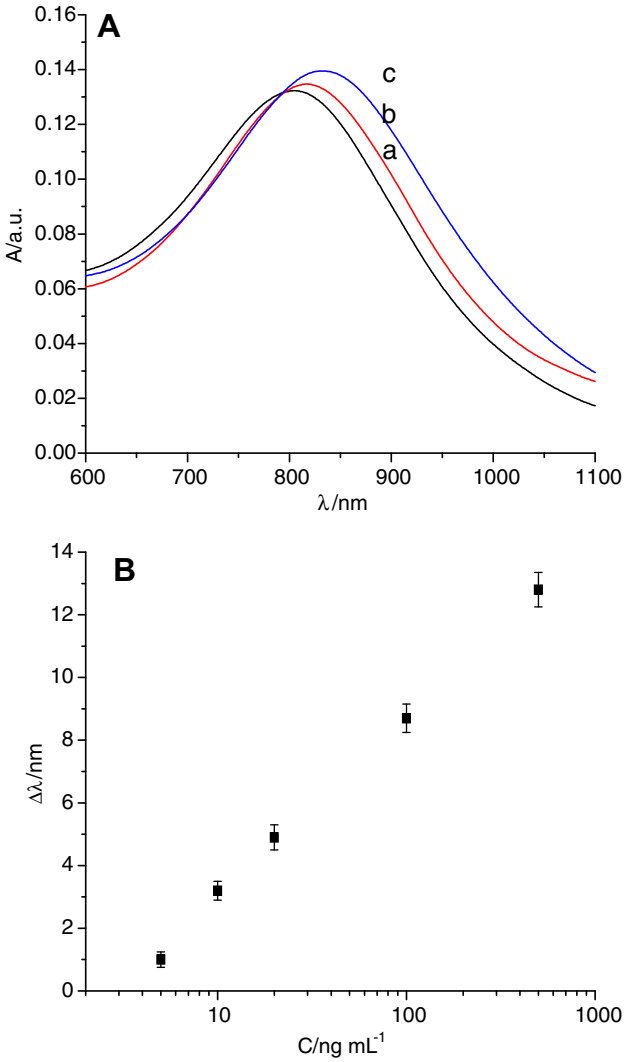

Fig. 6. UV–visible absorption spectra of HGNs before (a) and after incubated in goat anti-h-IgG (b), and binding of 500 ng/mL h-IgG (c) solution (A). Calibration curve for detection of h-IgG in solution at different concentration (B).

SA (1×10^{-6} M), an addition red-shift of ~36 nm was observed. Fig. 5B displays the response for the detection of SA in the solution. The sensor showed a linear response in the SA concentration range from 3×10^{-10} to 1×10^{-7} M.

The ITO/HGNs strips as LSPR-based biosensors were further validated by antibody-antigen binding investigation. Fig. 6A shows the LSPR shifts after each step of surface modification. The treatment of the ITO/HGNs strip with anti-h-IgG solution yielded a shift of 14 nm. The next step was the actual bioassay and involved the binding of the h-IgG onto anti-h-IgG. This binding interaction with 500 ng/mL of IgG provoked a further red-shift of ~13 nm. The calibration curve for detection of h-IgG in the solution at different concentration was shown in Fig. 6B. The reproducibility of biosensor was estimated from the determination of 100 ng/mL IgG at five different strips, with a R.S.D. 4.7%. The stability of the biosensor was also tested. No significant changes were found for measurement of 100 ng/mL IgG after storage at 4 °C for 20 days. The results indicate that the ITO/HGNs strip could be used to develop label-free immunological biosensors.

Conclusion

We have developed a simple synthetic route to fabricate hollow gold nanostructures onto the transparent ITO substrate. The LSPR

peak of HGNs was considerably red-shifted to ~800 nm as compared to the template of AgNPs. Moreover, the LSPR of HGNs exhibit a much more sensitive response toward environmental changes by compared with the AgNPs (template). These HGNs could be further functionalized special molecules due to clean surface of gold. Therefore, this novel approach could offer an opportunity to construct LSPR biosensors based on NIR HGNs.

Acknowledgments

This work was financially supported by the National Natural Science Foundation of China (No. 21075086), the Project of Scientific and Technologic Infrastructure of Suzhou (SZS201207) and the Priority Academic Program Development of Jiangsu Higher Education Institutions.

References

[1] B. Sepúlveda, P.C. Angelomé, L.M. Lechuga, L.M. Liz-Marzán, Nano Today 4 (2009) 244–251.
[2] M.E. Stewart, C.R. Anderton, L.B. Thompson, J. Maria, S.K. Gray, J.A. Rogers, R.G. Nuzzo, Chem. Rev. 108 (2008) 494–521.
[3] K.M. Mayer, J.H. Hafner, Chem. Rev. 111 (2011) 3828–3857.
[4] K.L. Kelly, E. Coronado, L.L. Zhao, G.C. Schatz, J. Phys. Chem. B 107 (2003) 668–677.
[5] M.B. Cortie, A.M. McDonagh, Chem. Rev. 111 (2011) 3713–3735.
[6] D. Wu, X. Xu, X. Liu, Solid State Commun. 146 (2008) 7–11.
[7] A.J. Haes, R.P. Van Duyne, Anal. Bioanal. Chem. 379 (2004) 920–930.
[8] H. Huang, X. Liu, B. Liao, P.K. Chu, Plasmonics 6 (2011) 1–9.
[9] J. Chen, Y. Chen, Anal. Bioanal. Chem. 399 (2011) 1173–1180.
[10] Y. Kim, T. Yu, E.C. Cho, Y. Ma, O.O. Park, Y. Xia, Angew. Chem. Int. Ed. 50 (2011) 6328–6331.
[11] P.K. Jain, X. Huang, I.H. El-Sayed, M.A. El-Sayed, Acc. Chem. Res. 41 (2008) 1578–1586.
[12] L.R. Hirsch, J.B. Jackson, A. Lee, N.J. Halas, J.L. West, Anal. Chem. 75 (2003) 2377–2381.
[13] V. Vongsavat, B.M. Vittur, W.W. Bryan, J.H. Kim, T.R. Lee, ACS Appl. Mater Interfaces 3 (2011) 3616–3624.
[14] Y. Wang, W. Qian, Y. Tan, S. Ding, Biosens. Bioelectron. 23 (2008) 1166–1170.
[15] M.M. Miller, A.A. Lazarides, J. Phys. Chem. B 109 (2005) 21556–21565.
[16] Q. Zhang, W. Wang, J. Goebl, Y. Yin, Nano Today 4 (2009) 494–507.
[17] Y. Sun, Y. Xia, Anal. Chem. 74 (2002) 5297–5305.
[18] S.E. Skrabalak, J. Chen, Y. Sun, X. Lu, L. Au, C.M. Cobley, Y. Xia, Acc. Chem. Res. 41 (2008) 1587–1595.
[19] H. Huang, C. He, Y. Zeng, X. Xia, X. Yu, P. Yi, Z. Chen, Biosens. Bioelectron. 24 (2009) 2255–2259.
[20] M. Fan, M. Thompson, M.L. Andrade, A.G. Brolo, Anal. Chem. 82 (2010) 6350–6352.
[21] Y. Shon, H.Y. Choi, M.S. Guerrero, C. Kwon, Plasmonics 4 (2009) 95–105.
[22] C. Wang, Z. Ma, T. Wang, Z. Su, Adv. Funct. Mater. 16 (2006) 1673–1678.
[23] M.H. Rashid, R.R. Bhattacharjee, T.K. Mandal, J. Phys. Chem. C 111 (2007) 9684–9693.
[24] I. Pastoriza-Santos, J. Pérez-Juste, L.M. Liz-Marzán, Chem. Mater. 18 (2006) 2465–2467.
[25] D. Wan, H. Chen, Y. Lin, S. Chuang, J. Shieh, S. Chen, ACS Nano 3 (2009) 960–970.
[26] Z. Zhang, Z. Yang, X. Liu, M. Li, L. Zhou, Scripta Mater. 63 (2010) 1193–1196.
[27] S. Bruzzone, M. Malvaldi, G.P. Arrighini, C. Guidotti, J. Phys. Chem. B 110 (2006) 11050–11054.